

# Fourier transform analysis of the spectral modulations obtained at the output of the uncompensated Michelson interferometer

PETR HLUBINA\*

Institute of Physics, Silesian University at Opava,  
Czech Republic

---

*The experimental demonstration of the spectral interference between two beams of a wide-spectrum source is presented at the output of the uncompensated Michelson interferometer. Three different modulations of the source spectrum with the wavelength-dependent periods of modulation affected by the group optical path difference (OPD) between both beams, in which the dispersion of the beam splitter is inscribed, are successfully processed using the Fourier transform analysis. Consequently, a good agreement between the experimental and the theoretical spectral modulations is achieved and the characteristics such as the unmodulated spectra, which agree well with those measured by blocking one of the arms of the interferometer, and the wavelength dependences of the group OPDs between both beams exceeding the source coherence length are obtained.*

---

## 1. Introduction

Optical interference plays a fundamental role in theoretical and experimental investigations of a large number of optical phenomena [1, 2]. The advantages of investigations of optical interference in the spectral domain are well known. These include, for example, the presence of the modulated (channelled) spectrum when the interference of two spatially completely coherent beams is considered [1], and the invention of the spectral changes of the radiated fields produced on interference of radiation from spatially partially coherent sources [2, 3]. The existence of the channelled spectrum means that the interference effects of light beams occur no matter how long or short the optical path difference (OPD) may be; the interference effect is reproduced as a spectral variation when the OPD is greater than the source coherence length [4-7]

and as a periodic spatial variation when the OPD is shorter than the source coherence length.

Theoretical and experimental investigations of the interference effects in the spectral domain have revealed their great impact on the progress of new optical diagnostics methods [4-11]. Thus the spectral modulation of both white and low-coherence light in a Michelson interferometer has been presented [4, 5] for measuring displacements ranging up to hundreds of micrometres. The spectral interference between two linearly polarized (LP) modes, which shows up a periodic modulation of the source spectrum resolved by a high-resolution spectrometer, has been used in the evaluation of the group-delay time difference between two LP modes [6, 7]. The real-time interferometric, high-precision measurement of the refractive index of a specimen as a function of the wavelength has been presented [8] from a single interferogram displayed in the spectral domain. White-light interferometry with channelled spectrum detection has been used in optical profilometry [9] and the use of dispersive white-light interferometers for absolute distance measurements,

---

\* address for correspondence: Petr Hlubina, Institute of Physics, Silesian University at Opava, Bezručovo nám. 13, 746 01 Opava, Czech Republic, e-mail: Petr.Hlubina@decsu.fpf.slu.cz

including effects of dielectric multilayer system, has been demonstrated [10, 11].

In this contribution, the mutual interference of two beams of a wide-spectrum source has been demonstrated experimentally in the spectral domain at the output of the uncompensated, that is dispersive, Michelson interferometer, when the group OPD between both beams exceeds the coherence length of the source. Thus, we have extended the use of a Michelson interferometer for the demonstration of the two-beam spectral interference experiment with a source whose spectrum is wider than that used in a previous work [5]. Consequently, we have obtained three different modulations of the source spectrum with the wavelength-dependent periods of modulation affected by the group OPD between both beams in which the dispersion of a beam splitter material is inscribed. Moreover, the Fourier transform analysis has been successfully applied to these three measured spectral modulations and good agreement between the experimental and the theoretical spectral modulations has been achieved and parameters such as the unmodulated spectra, which agree well with those measured by blocking one of the arms of the interferometer, and the wavelength dependences of the group OPDs have been obtained. It has also been demonstrated that the spectral modulations serve as an illustration of a technique for measuring the group OPDs ranging from approximately 100 to 400  $\mu\text{m}$ .

## 2. Experimental configuration

The experimental set-up used in the investigation of the spectral interference between two beams at the output of the uncompensated Michelson interferometer is

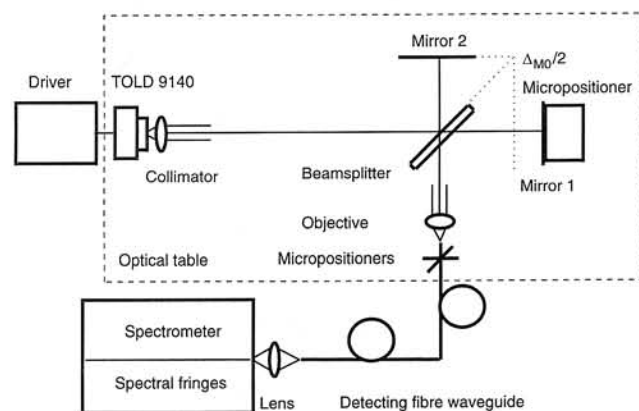


Fig. 1. Experimental set-up for the investigation of the spectral interference between two beams in the uncompensated Michelson interferometer.

shown schematically in figure 1. A Toshiba TOLD 9140 semiconductor laser diode (LD) operating below the threshold is used as a wide-spectrum source. This is due to a driver connected with the LD which enables us to control regimes of the LD and thus allows both the desired width of the spectrum and the output optical power of the LD to be obtained [12]. The LD with a collimator is used in a Michelson interferometer which consists of two mirrors and a beam splitter. The collimated beam from the LD is split at the beam splitter, giving two beams which travel different path lengths in two different arms of the interferometer so that at the output of the interferometer the OPD between both beams is  $\Delta_M(\lambda)$ . The wavelength dependence of the OPD results from different path lengths of both beams through the dispersive medium of a beam splitter. In other words, the Michelson interferometer is uncompensated. Beams are combined at the output of the interferometer giving for a suitable OPD, that is for the OPD shorter than the source coherence length, spatial interference fringes. When the OPD is substantially magnified, the spatial interference fringes disappear. The position of mirror 1 is controlled by a micropositioner which enable us to adjust the desired fine change in the OPD with nearly micrometre accuracy.

The Michelson interferometer configuration is placed on the optical table which supports a vibrational isolation. Because the spectrometer is placed in a different room from the Michelson interferometer configuration, a multimode fibre waveguide acting as the detecting fibre waveguide is used to launch the optical power from the output of the interferometer into the entrance slit of the monochromator. Moreover, the multimode fibre waveguide whose core diameter is approximately 200  $\mu\text{m}$ , and whose length is approximately 1 km, serves as a spatial filter. For the best operation of the measuring set-up it is crucial that no spatial integration of the interference fringes at the output of the interferometer is present. The state of the lowest spatial integration of the interference fringes can be easily inspected in a balanced Michelson interferometer when the OPD is zero and spatial interference fringes of the highest contrast are available at the output of the interferometer. A microscopic objective and micropositioners are used to launch the light from the interferometer into the detecting fibre waveguide in order to obtain the highest contrast of the optical pattern also at its output. The light from the detecting fibre waveguide is focused by a lens into a spectrometer [5, 7] comprising a Carl Zeiss SPM 2 grating monochromator (the variable width of its entrance slit enables the desired resolving power to be

adjusted), a semiconductor *p-i-n* photodetector with an amplifier and an IBM personal computer which create together with a chopper a computerized data acquisition and processing system utilizing the principle of synchronous detection. By this system the range of measured wavelengths, the wavelength step between two measurements as well as the time during which the data are averaged can be controlled.

### 3. Theoretical background

The mutual interference of two beams at an arbitrary point with transverse position vector  $\mathbf{R}$  at the output of the uncompensated Michelson interferometer is governed at the wavelength by the spectral interference law [2, 6]

$$S(\mathbf{R}; \lambda) = S_0(\mathbf{R}; \lambda) + S_1(\mathbf{R}; \lambda) + 2\sqrt{S_0(\mathbf{R}; \lambda) S_1(\mathbf{R}; \lambda)} \cos \left[ \frac{2\pi}{\lambda} \Delta_M(\mathbf{R}; \lambda) \right], \quad (1)$$

where  $S_0(\mathbf{R}; \lambda)$  and  $S_1(\mathbf{R}; \lambda)$  are contributions of both beams to the resultant spectral power density  $S(\mathbf{R}; \lambda)$ , and  $\Delta_M(\mathbf{R}; \lambda)$  is the spatially and spectrally dependent OPD between both beams at the output of the uncompensated Michelson interferometer. The dependence of the OPD  $\Delta_M(\mathbf{R}; \lambda)$  on the transverse position vector  $\mathbf{R}$  means that two superimposed and slightly tilted wavefronts of beams give rise at the output of the Michelson interferometer to interference fringes whose spatial frequency is determined by the tilt of the wavefronts, that is by the tilt of the mirrors. Similarly, the dependence of the OPD  $\Delta_M(\mathbf{R}; \lambda)$  on the wavelength means that two beams propagate on different path lengths through the dispersive medium of a beam splitter.

Let us consider now that the detecting fibre waveguide is used at the output of the Michelson interferometer to launch the optical power into a spectrometer. We assume that the spectrometer comprising input launching optics, grating monochromator, output optics and photodetector is characterized at the wavelength  $\lambda$  by the response function denoted as  $R(\lambda)$ . Spectral power at the output of the spectrometer can be expressed by the well-known convolution relation [6]

$$I(\lambda) = \iint S(\mathbf{R}; \lambda') A(\mathbf{R}) R(\lambda - \lambda') d^2 \mathbf{R} d\lambda', \quad (2)$$

where  $A(\mathbf{R})$  is the aperture function of the input end of the detecting fibre waveguide. The wavelength integration is performed over a wavelength range much larger than the width of the response function  $R(\lambda)$ . On sub-

stituting from equation (1) into equation (2), we obtain the most used form of the spectral interference law

$$I(\lambda) = I^{(0)}(\lambda) \left\{ 1 + V_I(\lambda) \cos \left[ \frac{2\pi}{\lambda} \Delta_M(\lambda) \right] \right\}, \quad (3)$$

where  $I^{(0)}(\lambda)$  is the reference spectral power, that is the reference spectrum, in which the effect of both the source spectrum and the response function of spectrometer is inscribed and  $V_I(\lambda)$  is the visibility of the measured spectral interference fringes in the two-beam interference experiment, in which the effect of both the spatial and the spectral integration as well as the effect of different contributions of both beams is included [5]. For the best operation of the measuring set-up it is desired that no spatial integration of the interference fringes by the input end of the detecting fibre waveguide is present (the highest visibility of the interference fringes can be achieved using the detecting fibre waveguide whose core diameter is small compared with the spatial period of interference fringes) and no spectral integration of the interference fringes by the spectrometer is present. One may conclude from equation (3) that the spectral modulation with the wavelength-dependent period of modulation

$$\Delta\lambda(\lambda) = -\frac{\lambda^2}{\Delta_M^g(\lambda)}, \quad (4)$$

is to be expected at the output of the spectrometer, if a spectrometer with a suitable resolution is used. Consequently, the highest visibility of the measured interference fringes can be achieved using a spectrometer whose width of response function  $R(\lambda)$  is small compared with the period of the spectral modulation. In equation (4),  $\Delta_M^g(\lambda)$  represents the group OPD between both beams in the uncompensated Michelson interferometer defined by the well-known relation

$$\Delta_M^g(\lambda) = \Delta_M(\lambda) - \lambda \frac{d\Delta_M(\lambda)}{d\lambda} \quad (5)$$

#### 3. 1. Fourier transform method of fringe pattern analysis

The Fourier transform method of fringe pattern analysis was originally conceived and demonstrated by Takeda *et al.* [13] for extracting phase information from a fringe pattern arising out of the interference of tilted wavefronts. The tilt between the interfering wavefronts determines the spatial carrier frequency of the spatial interferogram. Spectral interferograms, that



is spectral modulations, have the general form (3) which can be related to the similar form of one-dimensional spatial interferograms (the spatial coordinate is replaced by the wavelength) [13-15]

$$g(\lambda) = a(\lambda) + b(\lambda)\cos [2\pi f_0\lambda + \phi(\lambda)], \quad (6)$$

where  $a(\lambda)$  and  $b(\lambda)$  represent background and modulation terms respectively;  $f_0$  is the carrier frequency in the wavelength domain and  $\phi(\lambda)$  is the phase function.

Now we briefly review the Fourier transform method. Equation (6) may be rewritten

$$g(\lambda) = a(\lambda) + c(\lambda) \exp(i2\pi f_0\lambda) + c^*(\lambda)\exp(-i2\pi f_0\lambda) \quad (7)$$

where

$$c(\lambda) = \frac{1}{2}b(\lambda)\exp[i\phi(\lambda)], \quad (8)$$

and  $*$  denotes the complex conjugate. It follows from equation (8) that

$$b(\lambda) = 2|c(\lambda)|, \quad (9)$$

and

$$\tan\phi(\lambda) = \frac{\text{Im} [c(\lambda)]}{\text{Re} [c(\lambda)]} \quad (10)$$

Taking the Fourier transform of the fringe pattern with respect to  $\lambda$  gives

$$G(f) = A(f) + C(f-f_0) + C^*(-f-f_0), \quad (11)$$

where the capital letters denote Fourier spectra,  $f$  is the variable in the wavelength domain and  $C(f)$  is the Fourier transform of  $c(\lambda)$  with respect to  $\lambda$ . Since it is envisaged in practical applications that  $a(\lambda)$ ,  $b(\lambda)$  and  $\phi(\lambda)$  are slowly varying functions compared to the variations introduced by the carrier frequency  $f_0$ , the Fourier spectrum modulus consists of three distinct regions, corresponding to three terms in equation (11), separated by frequency  $f_0$ . The central d. c. spike and either of the two spectral side-lobes are filtered out leaving either  $C(f-f_0)$  or  $C^*(-f-f_0)$ . If  $C(f-f_0)$  is retained, and the inverse Fourier transform of this function is determined, then the result is the complex function  $c(\lambda)\exp(i2\pi f_0\lambda)$ . Multiplying by  $\exp(-i2\pi f_0\lambda)$  then gives  $c(\lambda)$ . The phase information  $\phi(\lambda)$  can be obtained using equation (10). The phase  $\phi(\lambda)$  so obtained is wrapped into the range from  $-\pi$  to  $\pi$  and has

to be corrected by using a phase-unwrapping algorithm [13-15].

## 4. Experimental results and discussion

Spectral powers or spectra are measured by a spectrometer whose resolving power results from the width adjustment of the entrance slit of a monochromator. In the usual operation of the spectrometer, the slit width is selected to be 300 m. The spectra are measured in the range of wavelengths from 675 to 705 nm with a 0.2 nm step between two measurements. The data are averaged for 1 s at each wavelength of measurement. Repeating measurements of spectra their reproducibility is confirmed.

Modulations of the source spectrum are measured at the output of the Michelson interferometer for the OPDs exceeding the source coherence length. Consequently, a balanced configuration of the Michelson interferometer is to be firstly adjusted. In the balanced configuration of the Michelson interferometer there are available at its output the spatial interference fringes of highest visibility. Now, if mirror 1 is shifted from the balanced interferometer configuration by the micropositioner, the visibility of the spatial interference fringes is reduced. If the total displacement, which is twice the actual displacement of the mirror, appreciably exceeds the coherence length, the spatial interference fringes disappear. For us it is the starting position from which the spectral interference between two beams will be studied at the output of the uncompensated Michelson interferometer.

Mirror 1 fixed with the micropositioner enables us to adjust for example three known and different positions for which the two-beam spectral interference can be confirmed. Denoting as  $\Delta_{M0}$  the initial OPD between both beams at the output of the Michelson interferometer, the corresponding OPD is magnified with a step of 100  $\mu\text{m}$  in a range of  $\Delta_{M0}$  to  $\Delta_{M0}+200 \mu\text{m}$ , which means that mirror 1 fixed with the micropositioner is displaced with a 50  $\mu\text{m}$  step between two measurements. Figures 2a)-2c) show by markers the corresponding measured normalized spectra. Corresponding theoretical normalized spectra resulting from spectral modulations given by equation (3) are also shown by full curves in figures 2a)-2c). We see good agreement between the theory and the experiment. We can also confirm that, in accordance with conclusions given in the previous work [5], the larger the OPD between both beams in the Michelson interferometer, the smaller is the period of spectral modulation and the lower is the visibility of the spectral interference fringes. The theoretical spectral

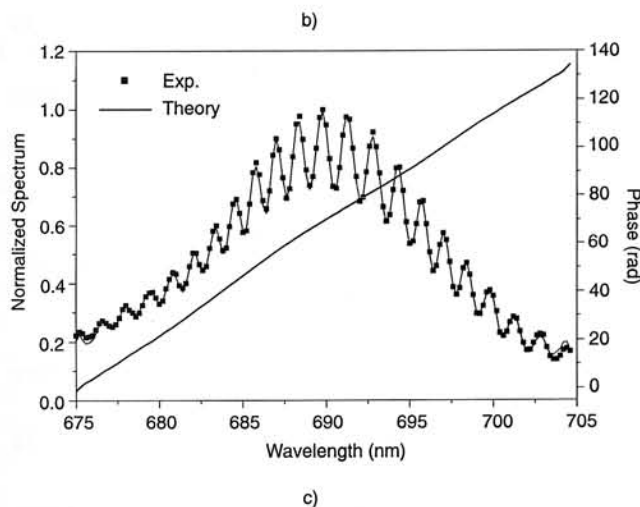
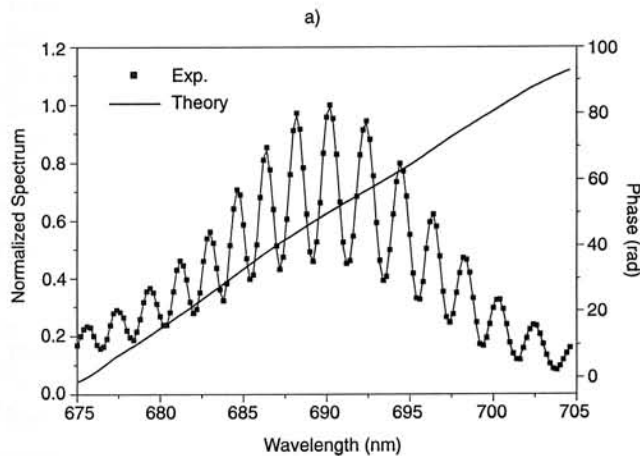
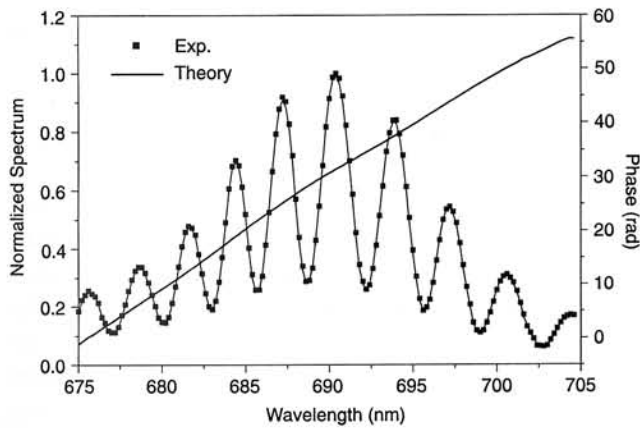


Fig. 2. Measured and theoretical normalized spectra together with the corresponding overall phases (bold curves) for three different optical path differences: a)  $\Delta M_0$ , b)  $\Delta M_0 + 100 \mu\text{m}$ , c)  $\Delta M_0 + 200 \mu\text{m}$ .

modulations are obtained by processing the measured spectral modulations using the Fourier transform method for the spectral fringe analysis that gives  $I^{(0)}(\lambda)$ ,  $V_I(\lambda)$  and  $\Delta M(\lambda)$ .

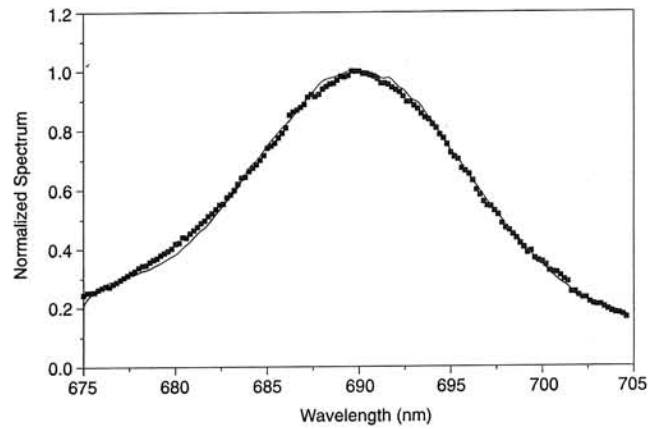


Fig. 3. Two unmodulated normalized spectra. The markers correspond to one blocked arm of the interferometer and the full line is obtained by processing the measured modulated spectrum shown in figure 2a).

Spectrum  $I^{(0)}(\lambda)$  or  $a(\lambda)$  in equation (6) is obtained as the inverse Fourier transform of the Fourier spectrum  $A(f)$ , where  $A(f)$  is obtained according to equation (11) by filtering  $G(f)$  leaving only  $A(f)$ . This procedure is demonstrated in figure 3, in which the corresponding unmodulated normalized spectrum  $I^{(0)}(\lambda)$  is compared with the spectrum obtained by blocking one of the arms of the interferometer. It can be seen that good agreement is present and a central wavelength  $\lambda_0$  of 689.6 nm as well as the full width at half maximum  $\Delta\lambda$  of 16 nm can be attributed to the spectrum of the TOLD 9140 laser diode. The corresponding coherence length  $l_c \approx \lambda_0^2/\Delta\lambda$  is 30  $\mu\text{m}$ .

The visibility of spectral interference fringes  $V_I(\lambda)$  can be easily obtained using equation (9) because  $b(\lambda)$  in equation (6) represents a product of the reference spectral power  $I^{(0)}(\lambda)$  and the visibility  $V_I(\lambda)$ . The Fourier transform method for the spectral fringe analysis presented in the previous section gives the overall phase  $\Phi(\lambda) = \Delta M(\lambda)2\pi/\lambda = 2\pi f_0\lambda + \phi(\lambda)$ . By processing the measured spectral modulations and using a phase-unwrapping algorithm the wavelength dependences of the overall phases  $\Phi(\lambda)$  for different OPDs are obtained. The wavelength dependences of the overall phases  $\Phi(\lambda)$  obtained from three measured spectral modulations are shown in figures 2a)–2c) by bold curves. All three curves are non-linear. This means that they are affected by the dispersion of a beam splitter.

From the wavelength dependences of the overall phases  $\Phi(\lambda)$ , the wavelength dependences of the OPDs and then using equation (5) the group OPDs can also be obtained. Fortunately, even if the overall phase  $\Phi(\lambda)$  and correspondingly the OPD  $\Delta M(\lambda)$  is known with ambiguity, it results from equation (5) that the group

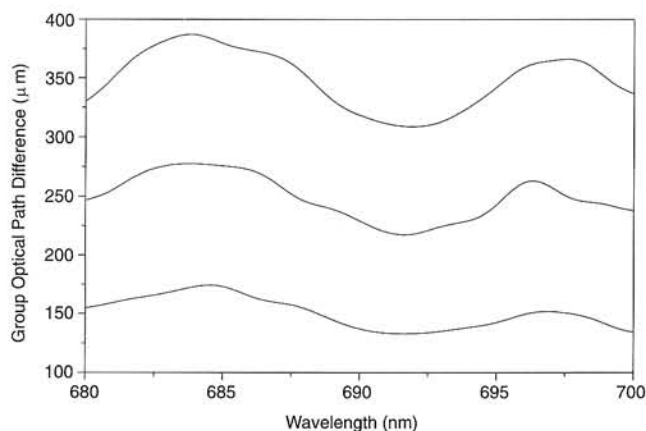


Fig. 4. The wavelength dependences of the absolute value of the group optical path differences between beams obtained by processing three modulated spectra shown in figures 2a)-2c).

OPD is not affected by it. The wavelength dependences of the absolute value of the group OPDs obtained from three measured spectral modulations shown in figures 2a)-2c) are depicted in figure 4. It is important to note that spectral region in which the group OPDs are considered is narrowed. This is owing to the phase evaluation errors near both edges of the spectral region [15] negatively affecting the group OPD evaluation errors. It can be seen from figure 4 that three wavelength dependences of the group OPDs, including two clearly resolved maxima, are similar. We should note that the evaluated wavelength dependences of the group OPDs can be compared with those resulting from the corresponding theory, including the dispersion of a beam splitter material, but this aspect is not considered in this paper. The wavelength dependences of the group OPDs shown in figure 4 can also be compared with those obtained by using the cross-correlation procedure [5, 16]. The cross-correlation between the measured and the theoretical spectral modulation is performed in the narrowed spectral regions, within which the group OPDs are considered to be spectrally independent [5]. Repeating this procedure over the whole measured spectral region the corresponding spectral dependence, which agrees well with that shown in figure 4, is obtained [16]. Finally, it is important to note that the separation of two neighbouring lines at a given wavelength can be used in the evaluation of the change in the group OPD. It is possible to perform a comparison of corresponding values with a value known from the change of the OPD associated with a known shift of mirror 1. Relatively

good agreement with the known value of 100  $\mu\text{m}$  is obtained at different wavelengths.

## 5. Conclusions

This paper clearly demonstrates the potential use of the Fourier transform method for obtaining an empirical dispersion curve of a beam splitter material from a single spectral interferogram. Three measured modulations of the source spectrum with the wavelength-dependent periods of modulation have successfully been processed using the Fourier transform method for the spectral fringe analysis and good agreement between the theoretical description of the two-beam spectral interference experiment and the measured spectral modulations has been achieved and parameters such as the unmodulated spectra, which agree well with those measured by blocking one of the arms of the interferometer, and the wavelength dependences of the group OPDs have been obtained.

## References

1. M. Born, E. Wolf: *Principles of Optics* (Pergamon Press, New York 1980).
2. L. Mandel, E. Wolf: *Optical Coherence and Quantum Optics* (Cambridge University Press, Cambridge 1995).
3. E. Wolf, D.F.V. James, Rep. Prog. Phys., **59** (1996) 771.
4. L.M. Smith, C.C. Dobson, Appl. Optics, **28** (1989) 3339.
5. P. Hlubina, J. Mod. Optics, **44** (1997) 1049.
6. P. Hlubina, J. Mod. Optics, **42** (1995) 2385.
7. P. Hlubina, J. Mod. Optics, **43** (1996) 1745.
8. C. Sáinz, P. Jourdain, R. Escalona, J. Calatroni, Optics Commun., **110** (1994) 381.
9. J. Schwider, L. Zhou, Opt. Lett., **19** (1994) 995.
10. U. Schnell, E. Zimmermann, R. Dändliker, Pure Appl. Opt., **4** (1995) 643.
11. U. Schnell, R. Dändliker, S. Gray, Opt. Lett., **21** (1996) 528.
12. D.A. Christensen, J. RotgE, A. Klemas, G. Loos, D. Merriman, Opt. Engng., **33** (1994) 2034.
13. M. Takeda, H. Ina, K. Kobayashi, J. Opt. Soc. Amer., **72** (1982) 156.
14. M. Takeda, Ind. Metrology, **1** (1990) 79.
15. R.J. Green, J.G. Walker, D.W. Robinson, Opt. Lasers Eng., **8** (1988) 29.
16. P. Hlubina, Proc. SPIE (in press).